Using weight functions in spatial point pattern analysis with application to plant ecology data

Lai Ping Ho and Sung Nok Chiu*

Department of Mathematics, Hong Kong Baptist University, Kowloon Tong, Hong Kong.

Abstract

A very common way of analyzing different and complicated plant behaviors is to use spatial point pattern analysis, which allows us to assess whether there is any structure present. To test the complete spatial randomness hypothesis, Diggle (1979) proposed a Monte Carlo test whose test statistic is the discrepancy between the estimated and the theoretical form of some summary function, such as the Ripley K-function. In this paper, we improve this test by adding various weight functions and get more powerful tests if decreasing and increasing weight functions are used for processes with short and long, respectively, range of interaction.

Keywords: K-function; Edge-correction; Complete Spatial Randomness; Monte Carlo simulation.

* Corresponding author. Email: snchiu@hkbu.edu.hk

1 Introduction

To understand the underlying processes of life history and population dynamics in plant ecology, spatial pattern analysis is a crucial statistical tool (Barot *et al.*, 1999; Dale and Powell, 2001; Haase, 1995; Lancaster and Downes, 2004; Perry *et al.*, 2002) for scientists because the plants of a given species can be described as discrete points in the region of interest. Spatial distribution of plants can reflect some of the possible processes, including establishment, growth, competition, reproduction, senescence and mortality, at work in the community. Therefore, applications of the spatial pattern analysis to ecological examples are abundant and include the determination of the spatial mortality patterns of, e.g., tropical forest (Sterner *et al.*, 1986), jack pine (Kenkel, 1988), kelp (Cole and Syms, 1999) and biennial plant (Suzuki *et al.*, 2003) and the behaviors of competition of, e.g., podocarp trees (Duncan, 1991) and desert shrub (Haase, 2001).

In general, the pattern of a given species in a plant community may be classified to be completely spatially random, clumped (aggregated or clustered) or dispersed (regular). Many elaborate and useful statistical methods (Dale and MacIsaac, 1989; Dale and Powell, 2001; Diggle, 2003; Greig-Smith, 1983; Ripley, 1976; Stoyan and Stoyan, 1994) have been developed to quantify the characteristics of spatial point patterns. The most popular summary statistic is the K-function introduced by Ripley (1976) and defined as

$$K(r) = \frac{\text{Average number of further plants within distance } r \text{ of an arbitrary plant}}{\lambda}, \quad r \geq 0,$$

where λ is the intensity of plants, or the average number of plants per unit area. Equivalently, taking a square root transformation proposed by Besag (1977) to stabilize the standard error

of its estimates leads to the L-function:

$$L(r) = r - \sqrt{\frac{K(r)}{\pi}}.$$

Theoretically, for a Poisson process, the value of $K(r)$ is equal to πr^2 (Dale, 1999, p.215), and so $L(r) = 0$. Note that some authors write $L(r) = \sqrt{K(r)/\pi} - r$ and some write $L(r) = \sqrt{K(r)/\pi}$. However, for exploratory analyses, Diggle (2003, p. 56) suggested to plot $K(r)$ or $K(r) - \pi r^2$ because of its direct physical interpretation in terms of counting numbers of events in circular regions.

Such a summary function can be used to construct statistics for testing the complete spatial randomness (CSR) hypothesis and a most popular one is

$$\sup_{r \le r_0} \left| r - \sqrt{\frac{\hat{K}(r)}{\pi}} \right|, \tag{1}$$

where r_0 is a suitably chosen upper limit and $\hat{K}(r)$ is an estimator of $K(r)$ (Diggle, 1979). We have the upper limit r_0 because as the value r increases, the variance of the test statistics increases, leading to higher type II error rate. Thus, we have to, somewhat arbitrarily, set an *a priori* cutoff point r_0 for the range of r. In fact, the use of the upper limit r_0 can be regarded as multiplication by a zero-one weight function $\mathbf{1}_{[0,\, r_0]}(\cdot)$, where

$$\mathbf{1}_{[0,\, r_0]}(x) = \begin{cases} 1, & 0 \le x \le r_0, \\ 0, & \text{otherwise}, \end{cases}$$

so that the test statistic in formula (1) can be expressed as

$$\sup_{r} \left\{ \left| r - \sqrt{\frac{\hat{K}(r)}{\pi}} \right| \cdot \mathbf{1}_{[0, r_0]}(r) \right\}. \tag{2}$$

Although there have been some recommendations (Diggle, 2003, p. 87; Ripley, 1979) for the value of r_0, the reason for using a zero-one weight function instead of other weight

functions has not been addressed. In this paper, we consider other weight functions and investigate their corresponding powers in testing the CSR hypothesis. Because the mean and the standard error of the difference $\left| r - \sqrt{\hat{K}(r)\pi} \right|$ are not constant functions of r, different upper limit r_0 will lead to different critical values (Chiu, 2007) and different powers (Ho and Chiu, 2006) and so consequently it is natural to expect different powers for weight functions of different shape.

2 Methodology

2.1 The K-function

As mentioned above, $K(r)$ is defined as the ratio of the expected number of plants within distance r of a randomly chosen plant to the intensity λ. Suppose that we observe n plants over a particular region W of area A, and let u_{ij} be the distance between plants i and j. It seems that the empirical mean $\frac{\sum_{i=1}^{n}\sum_{i\neq j}^{n}\mathbf{1}_{[0,r]}(u_{ij})}{n}$ would be a natural estimator of the theoretical mean $\lambda K(r)$. However, the estimation of this average is intervened by the edge-effects because the plant patterns are observed via a bounded sampling window W. Some unobserved plants may be within distance r of an observed plant lying close to the boundary of the window. As a result, this empirical mean underestimates the true $\lambda K(r)$. Various edge-corrected estimators have been proposed in the literature. Two standard edge-corrected estimators, which are empirical weighted average, of the theoretical mean $\lambda K(r)$ are

$$\widehat{\lambda K}_{\text{trans}}(r) = \frac{\sum_{i=1}^{n}\sum_{i\neq j}^{n}\theta_{ij}^{-1}\mathbf{1}_{[0,r]}(u_{ij})}{n},$$

$$\widehat{\lambda K}_{\text{iso}}(r) = \frac{\sum_{i=1}^{n}\sum_{i\neq j}^{n} w_{ij}^{-1}\mathbf{1}_{[0,r]}(u_{ij})}{n},$$

where θ_{ij} is the ratio of overlapping area of W and W_{j-i} to the area of W, $W_j = W+j = \{i+j: i \in W\}$ and w_{ij} is the proportion of circumference of the circle centered at the i-th plant with radius u_{ij}. The corresponding edge-correction method of the estimates $\widehat{\lambda K}_{\text{trans}}(r)$ and $\widehat{\lambda K}_{\text{iso}}(r)$ are called translational edge-correction and isotropic edge-correction, respectively. see Ripley (1988) and Stoyan and Stoyan (1995) for details. If we divide an estimator of $\lambda K(r)$ by n/A, which is a natural estimator of the intensity λ, we get an estimator of $K(r)$.

2.2 Statistical Test

We multiply the zero-one weight function in formula (2) by a weight function w and get

$$\sup_r \left(\left| r - \sqrt{\frac{\hat{K}(r)}{\pi}} \right| \cdot \mathbf{1}_{[0,r_0]}(r) \cdot w(r) \right), \tag{3}$$

which hereinafter is called the maximum statistic. Another popular measure of discrepancy is the integral

$$\int_0^{r_0} \left(r - \sqrt{\frac{\hat{K}(r)}{\pi}} \right)^2 \mathrm{d}r = \int_0^{\infty} \mathbf{1}_{[0,r_0]}(r) \left(r - \sqrt{\frac{\hat{K}(r)}{\pi}} \right)^2 \mathrm{d}r.$$

(Cressie, 1993, Eq. (8.4.23); Diggle, 2003, e.g. Eq. (2.7), (2.10), (2.14); Thönnes and van Lieshout, 1999; Yamada and Rogerson, 2003). Thus, multiplying $\mathbf{1}_{[0,r_0]}$ by w, we have

$$\int_0^{\infty} w(r)\mathbf{1}_{[0,r_0]}(r) \left(r - \sqrt{\frac{\hat{K}(r)}{\pi}} \right)^2 \mathrm{d}r, \tag{4}$$

which hereinafter is called the integral statistic. A usual weight function to stabilize the variance is the reciprocal of standard deviation of $\hat{L}(r)$, $w_1(r) = \dfrac{1}{\sqrt{\mathrm{var}(\hat{L}(r))}}$, which can

be estimated by the variance of $\hat{L}(r)$ from m simulated patterns at the same value of r, and then took the reciprocal of the standard deviation of $\hat{L}(r)$ to get pointwise the weight function w_1. In addition, six more weight functions, $w_2(r) = \exp(-r)$, $w_3(r) = 10^{-r}$, $w_4(r) = 1 - 2r$, $w_5(r) = r$, $w_6(r) = \exp(r) - 1$ and $w_7(r) = r\exp(-r)$, are deliberated to compare with the degenerate weight function $w_0(r) \equiv 1$. These functions are chosen as representatives because they include increasing and decreasing functions that changes linearly or exponentially. Intuitively, because the standard deviation of $\hat{L}(r)$ is increasing, we expect that decreasing functions, such as w_2, w_3 and w_4, will lead to more powerful statistics and increasing functions, such as w_5, w_6 and w_7, will worsen the performance.

In our simulation study, the CSR hypothesis was tested against two alternative models, namely, the conditional Poisson cluster process and the Strauss process with n points each.

Conditional Poisson cluster process: The idea is to place a cluster of points (daughters) around each point (parent) of an invisible stationary Poisson process. More precisely, first, n_c independent invisible parents are distributed uniformly in a unit square and then n daughters are assigned randomly to these parents and such that each daughter is located uniformly in a bounded region B centered at her parent under the periodic boundary condition, i.e. the square is converted into a torus. We consider isotropic cluster processes in which the bounded regions B are disks with radius R.

Strauss process: It is a pairwise interaction point process that produces, by self-inhibiting, patterns in which plants are more spread out than they would be in CSR; such patterns exhibit regularity. We start with a Poisson process in a bounded region and then define the Strauss process $\{\mathbf{x}_1, \mathbf{x}_2, \ldots\}$ by giving a probability density with respect to the Poisson

process. The probability density of the Strauss process is proportional to $\Pi_{\mathbf{x}_i,\mathbf{x}_j} c^{\mathbf{1}_{[0,R]}(\|\mathbf{x}_i-\mathbf{x}_j\|)}$ so that the parameter c controls the strength of inhibition and the parameter R determines the range of inhibition in such a way that $c = 0$ and $c = 1$ correspond to the hard core process with hard core distance R and the Poisson process, respectively; for $0 < c < 1$ we have a self-inhibiting point process. For details, see Kelly and Ripley (1976) and Strauss (1975).

For each alternative, we performed s times the Monte Carlo test suggested by Diggle (1979) to estimate the power: the CSR hypothesis would be rejected whenever the test statistic calculated from a pattern generated according to the alternative model, when pooled together with the values of the same statistic calculated from m simulated patterns of a binomial process in which an equal number of independent plants are uniformly distributed in the study region, has been ranked in the top 5%. The binomial process is in fact a conditional Poisson process, given the number of plants in the study region is fixed. In our simulation study, we performed $s = 100$ times (Chiu, 2003; Diggle, 1979; Ho and Chiu, 2006; Thönnes and van Lieshout, 1999) the Monte Carlo test and simulated $m = 99$ patterns (Cressie, 1993, p. 636; Diggle, 2003, p. 9; Haase, 1995; Kenkel, 1993; Stoyan and Stoyan, 1994, p. 301) of binomial process. These $m = 99$ patterns will also be the patterns used to estimate the variance of $\hat{L}(r)$ for the weight function w_1.

3 Simulation

To compare the efficacy of adding various weight functions, each of the seven weight functions and the two edge-corrected estimators mentioned above was employed in the test statistics

given in formulae (3) and (4). Two sample sizes $n = 25$ and $n = 100$ were chosen for simulation to represent small and large samples. The choice of the upper limit r_0 is arbitrary but important, and a suitably chosen upper limit r_0 can yield more powerful tests. Consider that the study region is a unit square and $w(r) = w_0(r)$. Diggle (2003, p. 87) recommended that the upper limit r_0 should be at most 0.25. Also, Ripley (1979) suggested $r_0 = 0.25$ for $n = 25$ and $r_0 = 0.125$ for $n = 100$, i.e. r_0 is inversely proportional to $\sqrt{n}$. The estimated powers of the maximum statistic and the integral statistics with different weight functions against the conditional Poisson cluster process and the Strauss process with various parameter values are given, as functions of r_0, in Figures $1 - 8$, from which we have the following conclusions.

To measure the discrepancy, neither the L_∞-norm, corresponding to the maximum statistic, nor the L_2-norm, corresponding to the integral statistic, is uniformly better than the other in the examples covered. The situation is similar to the Kolmogorov–Smirnov statistic and the Cramér–von Mises statistic in goodness of fit test.

The natural weight function w_1 for variance stabilization apparently works not better than w_0, especially against the Strauss point process, even though its powers, unlike those of w_0, do not drop substantially when r increases in the case of the maximum statistics and are so close to those of other weight functions in the case of the integral statistics. Hence, it is not worthwhile to consider this computationally messy weight function, and so let us focus on other weight functions introduced in Section 2.2.

For the Strauss process, obviously, we can observe that no matter which weight function was used in either the maximum or the integral test statistic, the estimated powers decrease as the value of r_0 increases. Also, we can find that the results of both test statistics with the

decreasing functions w_2, w_3 and w_4 (solid lines) usually give higher estimated power than those with w_0. Despite the fact that the values of the estimated power by using the integral statistic with different weight functions are so close to each other, the results of those tests with w_4 usually show the highest power and the same conclusions can be drawn from the maximum statistic.

Besides, as r_0 increases, the estimated powers of the maximum statistic with w_3 and w_4 nearly remain unchanged, and that with w_2 just descends slightly, whereas that with w_0 drops rapidly, especially for $n = 100$. This situation reminds us the important role of a suitably chosen upper limit r_0 plays, and a low power test will be resulted from a poorly chosen r_0. We can observe from Figures $1 - 4$ that the estimated powers are not always the highest at the values of r_0 recommended by Ripley (1976).

Consider the dashed lines, corresponding to the increasing weight functions w_5, w_6 and w_7, in Figures $1 - 4$, they do not work very well; that is what we expected. However, when we study Figures $5 - 8$ for cluster processes, we can find, strikingly, that the conclusions for the cluster and the Strauss processes are in the reverse directions; the decreasing weight functions will worsen the situation when we test against the Poisson cluster process.

This seemingly paradoxical phenomenon can be explained by the choice of the value of the parameter R; note that the choice of the parameter R cannot be too arbitrary because the estimated powers become larger, and quickly approach 100%, when R increases in a regular process or when R decreases in a cluster process. Conversely, the powers become smaller, and quickly approach 0%, when R decreases and increases in a regular process and a cluster process respectively. Thus, we should not use too large or too small values of R

to simulate different processes, otherwise we cannot compare the performance of different weight functions. We have considered a lot of different values of parameters in each process, including c ranged from 0 to 0.5 with R ranged from 0.04 to 0.1 for regular patterns, and n_c ranged from 5 to 50 with R ranged from 0.075 to 0.5 for clustered patterns. All of them led to the same conclusions obtained above. How the difference in these ranges of R and the upper bound $r_0 \leq 0.25$ caused the paradoxical observation would be explained as follows.

We can see that the powers, as functions of r_0, attain their maxima around $r_0 = R$. Since, for the Strauss processes the values of R are small, the powers in Figures $1 - 4$ show mainly a decreasing pattern. In contrast, the values of R are large for the cluster processes and so the powers in Figures $5 - 8$ show mainly an increasing pattern; if we allow a larger r_0, we can see that the powers will go down after $r_0 = R$ (Figure 10).

Figure 1 about here

Figure 2 about here

Figure 3 about here

Figure 4 about here

Figure 5 about here

Figure 6 about here

Figure 7 about here

Figure 8 about here

In fact, as we can see from Figures 9 and 10, the difference in the performance of the weight functions does not come from the clustered or regular nature of the alternative models but come from the difference in the range of interaction. Moreover, in Figures 9 and 10 we introduce four more decreasing functions, $w_8(r) = \exp(-\sqrt{r})$, $w_9(r) = \exp(-r^2)$, $w_{10}(r) = 1 - \sqrt{2r}$, $w_{11}(r) = 1 - 4r^2$, and five more increasing functions $w_{12}(r) = \sqrt{r}$, $w_{13}(r) = r^3$, $w_{14}(r) = \exp(\sqrt{r}) - 1$, $w_{15}(r) = \exp(r^2) - 1$ and $w_{16}(r) = r\exp(-\sqrt{r})$, so that we have more different rates of change for comparison. Since we do not have any closed expressions of the integral statistic for some of these weight functions, we only consider the maximum statistic. Allowing us to obtain the exact statistic value for any arbitrary weight function is an advantage of the maximum statistic. We do not, however, mean that numerical approximation for the integral statistic will lead to less powerful tests.

Figure 9 about here

Figure 10 about here

The various weight functions suggested in this paper apparently show different performance. Figure 11 illustrates the increase/decrease rates of different weight functions. For a long range of interaction, w_7, w_{12}, w_{14} and w_{16} which are convex upwards functions, perform better than the other increasing weight functions which are concave upwards functions, in most cases. Conversely, using a decreasing weight function is preferable for a short range of interaction. The decreasing weight functions w_3, and w_{10} which are convex downwards functions with higher decrease rate, and the linear decreasing weight function w_4 with higher decrease rate work better than the other decreasing weight functions. It may be possible

that the shape of a weight function will affect the power of the test statistic but we do not have strong evidence.

Figure 11 about here

Consider a Strauss process with $n = 25$, $c = 0.4$ and $R = 0.2$, which is shown in Figure 9, in which, we plot the powers up to $r_0 = 0.5$ even though Diggle suggested that at most $r_0 = 0.25$. We can observe that the increasing weight functions give the maximum powers and have a higher power than the decreasing weight functions at $r_0 = R$. This observation, which compared with the conclusion obtained from Figures $1 - 8$, reinforces the claim that it is not the clustered or regular nature but the range of interaction that matters.

Hence, if a short range of interaction is suspected or hypothesized, we should use a decreasing weight function, whilst if a long range of interaction is suspected or hypothesized, use an increasing weight function with a suitably chosen r_0, say, the suspected range of interaction or the recommendation by Ripley.

A plausible explanation for this interesting phenomenon is as follows. We would like to have a weight function that assigns heavier weights to the differences around the true range of interaction, say R, but of course there is no such a magic function for all kinds of patterns. For a small R, a decreasing weight function will assign lighter weights to differences at larger $r > R$, which are not as informative as the differences around R and have larger standard errors. For a large R, an increasing weight function will assign lighter weights to differences at smaller $r > R$, which again are not as informative as the differences around R. However, it also, undesirably, assigns heavier weights to differences at larger $r > R$, where the standard errors are larger. Nevertheless, we have the upper limit r_0, which will assign

zero weight to differences at $r > r_0$. Thus, in either case we should be able to have heavier (but not the heaviest) weights assigned to the most informative differences and lighter weight to differences that are either less informative or have very large standard errors.

In application, a pair correlation function can be used to check the range of interaction. It can also help us check if the conclusion is consistent with the capacity of that weight function.

4 Real Data

Figure 12(a) shows the locations of trees in a 75m $\times$ 75m region of broad-leaved multispecies old-growth forest in the south-east of Central Russia (Smirnova, 1994), excluding the trees which are fully overshadowed by neighboring trees. When we rescale the study region to a unit square, the value recommended by Ripley (1979) of r_0 for 270 points should be 0.0761, which is rather small.

Figure 12 about here

Grabarnik and Chiu (2002) indicated that their Q^2-statistic provides strong evidence against the CSR hypothesis (p-value = 0.0041) for these data. In our approach, first of all, we estimate the pair correlation function g which is shown in Figure 12(b), from which we found that the empirical g suggests that the range of interaction may be long, so that increasing weight functions may be used.

We obtained the Monte Carlo p-values for the maximum statistics using different edge-corrections and different weight functions on the basis of 99 independent realizations of the

binomial process with the same number of points ($n = 270$). The plots of estimated p-value are given in Figure 13. We should consider the test statistics with increasing weight functions, from which at the recommended value of r_0 (0.0761), we have strong evidence to reject the CSR at the 0.05 significance level by using any one of the two edge correction mentioned above. Only dashed lines (increasing weight function) are below the significance level around the recommended r_0. The p-values obtained by using other weight functions, including the degenerate weight function w_0, do not suggest rejection. That is to say, only if our recommendation is followed, we are able to reach the same conclusion as that documented in another study.

Figure 13 about here

Acknowledgements

This research was supported by grants from the Research Grants Council of the Hong Kong Special Administrative Region, China (Project Nos. HKBU2048/02P and HKBU200503) and an FRG grant of the Hong Kong Baptist University. I thank the referee for helpful comments.

References

Barot, S., Gignoux, J., Menaut, J. C. (1999). Demography of a savanna palm tree: predictions from comprehensive spatial pattern analyses. *Ecology* **80**:1987-2005.

Besag, J. (1977). Contribution to the discussion of Dr Ripley's paper. *Journal of the Royal Statistical Society Series B* **39**:193-195.

Chiu, S. N. (2003). Spatial point pattern analysis by using Voronoi diagrams and Delaunay tessellations — a comparative study. *Biometrical Journal* **45**:367-376.

Chiu, S. N. (2007). Correction to Koen's critical values in testing spatial randomness. *Journal of Statistical Computation and Simulation* **77**:1001-1004.

Cole, R. G., Syms, C. (1999). Using spatial pattern analysis to distinguish causes of mortality: an example from kelp in north-eastern New Zealand. *Journal of Ecology* **87**:963-972.

Cressie, N. A. C. (1993). *Statistics for Spatial Data. Revised ed.* New York: Wiley.

Dale, M. R. T., MacIsaac, D. A. (1989). New methods for the analysis of spatial pattern in vegetation. *Journal of Ecology* **77**:78-91.

Dale, M. R. T. (1999). *Spatial Pattern Analysis in Plant Ecology.* Cambridge: Cambridge University Press.

Dale, M. R. T., Powell, R. D. (2001). A new method for characterizing point patterns in plant ecology. *Journal of Vegetation Science* **12**:597-608.

Diggle, P. J. (1979). On parameter estimation and goodness-of-fit testing for spatial point patterns. *Biometrics* **35**:87-101.

Diggle, P. J. (2003). *Statistical Analysis of Spatial Point Patterns.* 2nd ed. London: Arnold.

Duncan, R. P. (1991), Competition and the coexistence of species in a mixed podocarp stand. *Journal of Ecology* **79**:1073-1084.

Grabarnik, P., Chiu, S. N. (2002). Goodness-of-fit test for complete spatial randomness against mixtures of regular and clustered spatial point processes. *Biometrika* **89**:411-421.

Greig-Smith, P. (1983). *Quantitative Plant Ecology.* Oxford: Blackwell Scientific Publica-

tions.

Haase, P. (1995). Spatial pattern analysis in ecology based on Ripley's K-function: introduction and methods of edge correction. *Journal of Vegetation Science* **6**:575-582.

Haase, P. (2001). Can isotropy vs. anisotropy in the spatial association of plant species reveal physical vs. biotic facilitation? *Journal of Vegetation Science* **12**:127-136.

Ho, L. P., Chiu, S. N. (2006). Testing the complete spatial randomness by Diggle's test without an arbitrary upper limit. *Journal of Statistical Computation and Simulation* **76**:585-591.

Kelly, F. P., Ripley, B. D. (1976). A note on Strauss's model for clustering. *Biometrika* **63**:357-360.

Kenkel, N. C. (1988). Pattern of self-thinning in jack pine: testing the random mortality hypothesis. *Ecology* **69**:1017-1024.

Kenkel, N. C. (1993). Modeling Markovian dependence in populations of aralia nudicaulis. *Ecology* **74**:1700-1706.

Lancaster, J., Downes, B. J. (2004). Spatial point pattern analysis of available and exploited resources. *Ecography* **27**:94-102.

Perry, J. N., Liebhold, A. M., Rosenberg, M. S., Dungan, J., Miriti, M., Jakomulska, A., Citron-Pousty, S. (2002). Illustrations and guidelines for selecting statistical methods for quantifying spatial pattern in ecological data. *Ecography* **25**:578-600.

Ripley, B. D. (1976). The second-order analysis of stationary processes. *Journal of Applied Probability* **13**:255-266.

Ripley, B. D. (1979). Tests of 'randomness' for spatial point patterns. *Journal of the Royal*

Statistical Society Series B **41**:368-374.

Ripley, B. D. (1988). *Statistical inference for spatial processes.* Cambridge: Cambridge University Press.

Smirnova, O. V. (Ed.) (1994). *East-European Broad-leaved Forests* (in Russian). Moscow: Nauka.

Sterner, R. W., Ribic, C. A., Schatz, G. E. (1986). Testing for life historical changes in spatial patterns of four tropical tree species. *Journal of Ecology* **74**:621-633.

Stoyan, D., Stoyan, H. (1994). *Fractals, Random Shapes and Point Fields: Methods of Geometrical Statistics.* New York: Wiley.

Stoyan, D., Kendall, W. S., Mecke, J. (1995). *Stochastic Geometry and its Applications.* Chichester: Wiley.

Strauss, D. J. (1975). A model for clustering. *Biometrika* **62**:467-475.

Suzuki, R. O., Kudoh, H., Kachi, N. (2003). Spatial and temporal variations in mortality of the biennial plant, *Lysimachia rubida*: effects of intraspecific competition and environmental heterogeneity. *Journal of Ecology* **91**:114-125.

Thönnes, E., van Lieshout, M. C. (1999). A comparative study on the power of van Lieshout and Baddeley's J-function. *Biometrical Journal* **41**:721-734.

Yamada, I., Rogerson, P. A. (2003). An empirical comparison of edge correction methods applied to K-function analysis. *Geographical Analysis* **35**:97-109.

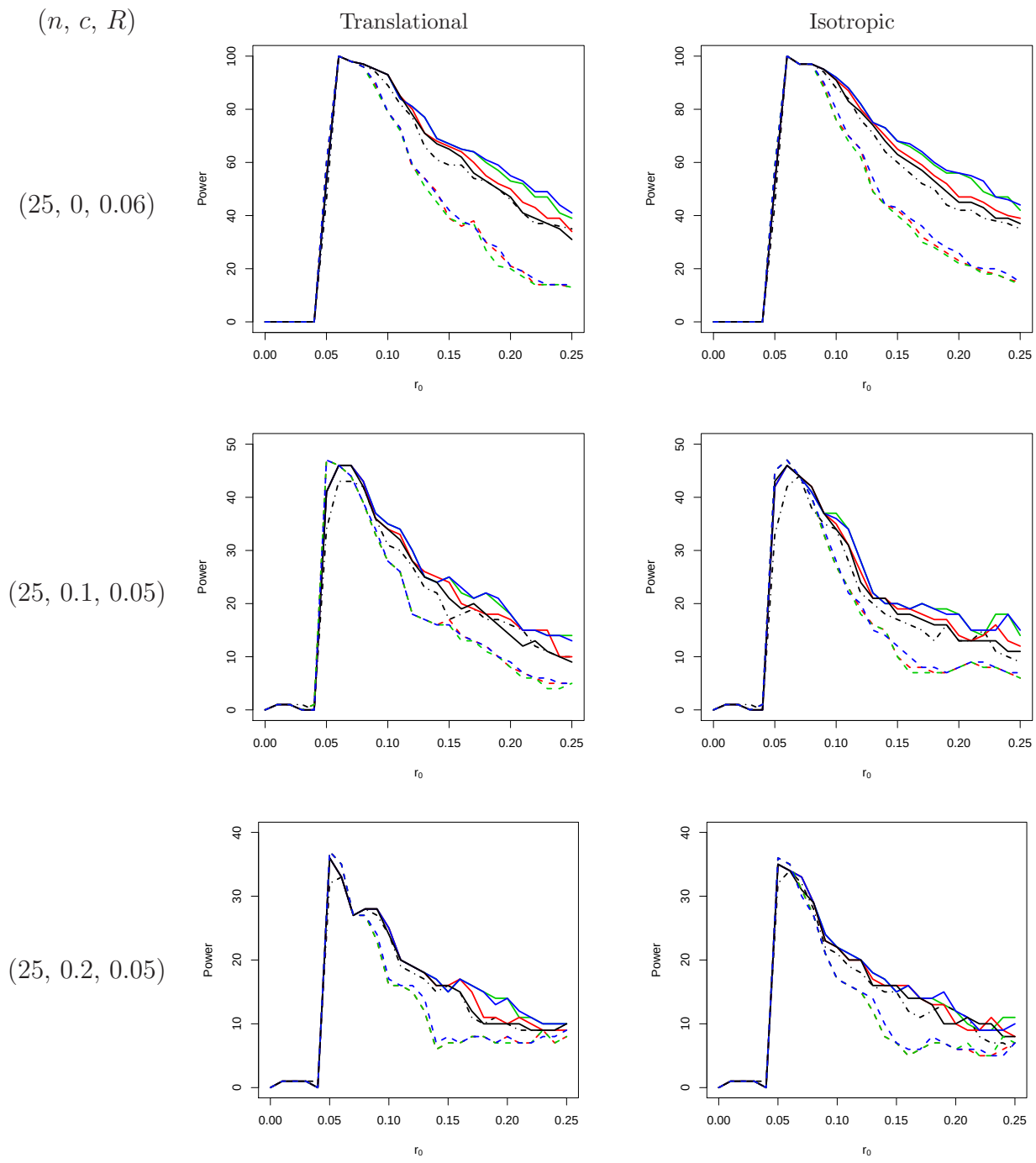

Figure 1: Estimated power (in percent) of the integral statistic for testing CSR against Strauss processes with 25 points, where c is the parameter that controls the strength of interaction and R is the range, in a unit square by the translational edge-correction and the isotropic edge-correction with eight weight functions (——, w_0; $\cdots\cdots$, w_1; ——, w_2; ——, w_3; ——, w_4; – – –, w_5; – – –, w_6; – – –, w_7).

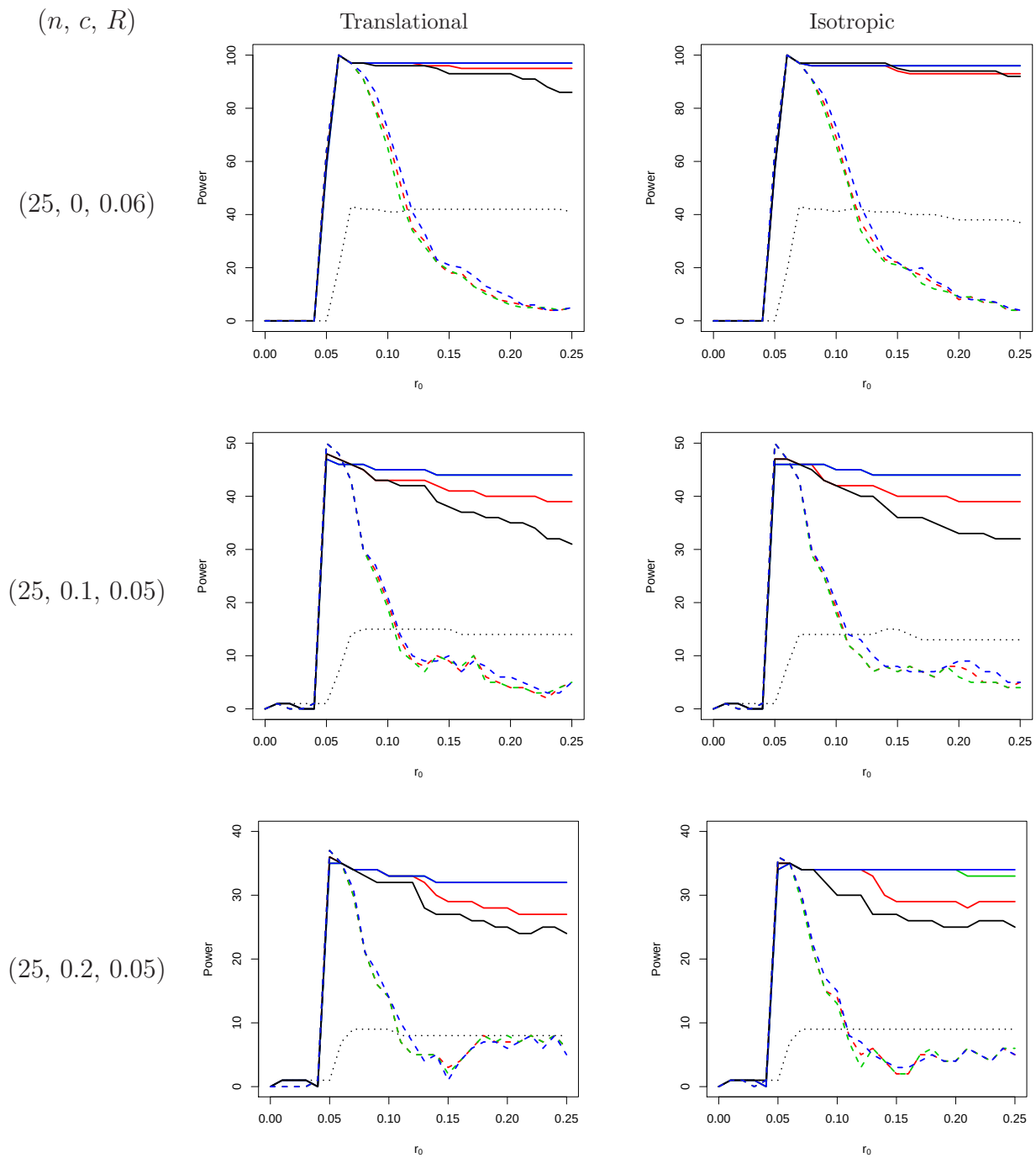

Figure 2: Estimated power (in percent) of the maximum statistic for testing CSR against Strauss processes with 25 points, where c is the parameter that controls the strength of interaction and R is the range, in a unit square by the translational edge-correction and the isotropic edge-correction with eight weight functions (———, w_0; $\cdots\cdots$, w_1; ———, w_2; ———, w_3; ———, w_4; – – –, w_5; – – –, w_6; – – –, w_7).

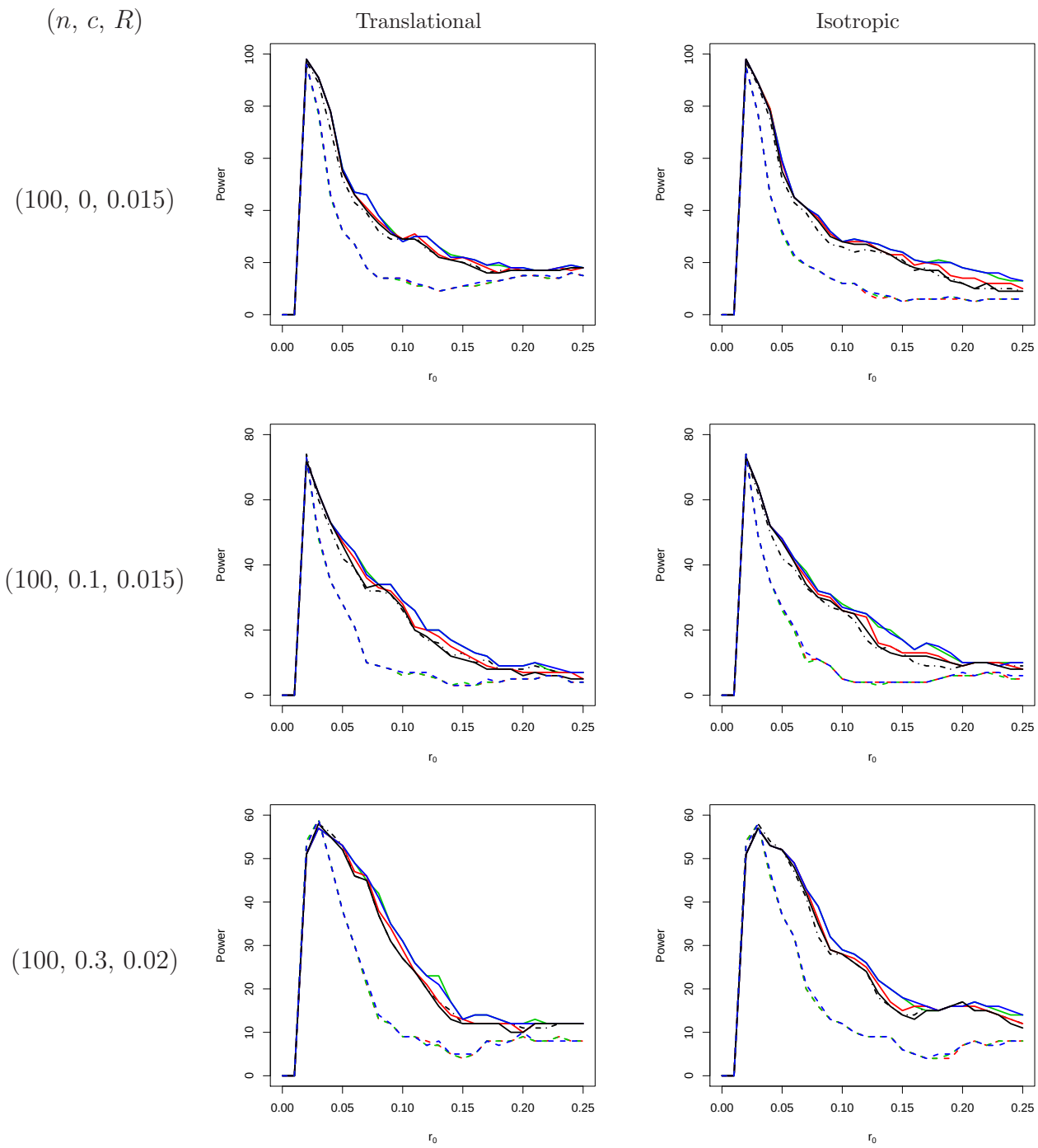

Figure 3: Estimated power (in percent) of the integral statistic for testing CSR against Strauss processes with 100 points, where c is the parameter that controls the strength of interaction and R is the range, in a unit square by the translational edge-correction and the isotropic edge-correction with eight weight functions (———, w_0; $\cdots\cdots$, w_1; ———, w_2; ———, w_3; ———, w_4; – – –, w_5; – – –, w_6; – – –, w_7).

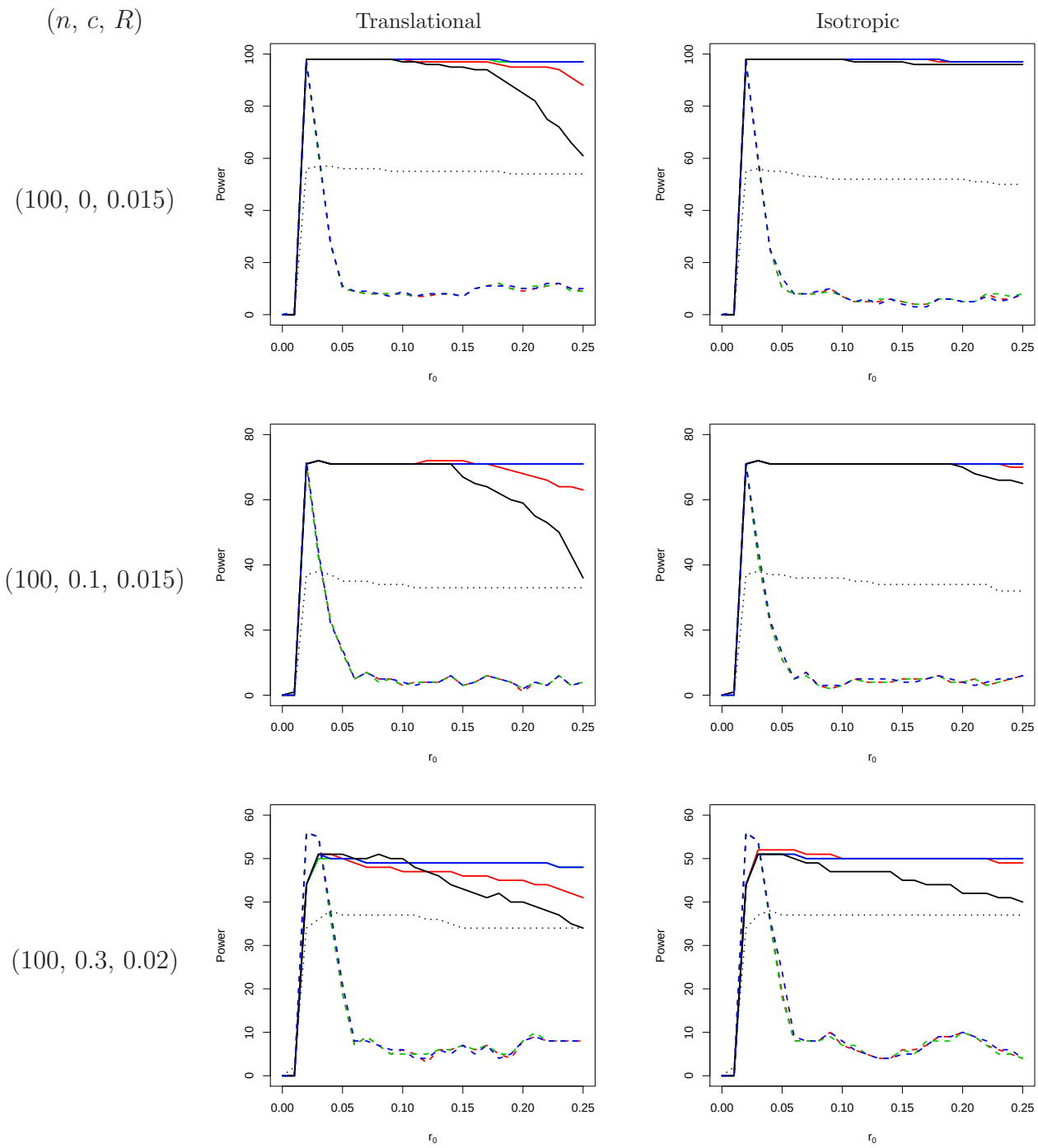

Figure 4: Estimated power (in percent) of the maximum statistic for testing CSR against Strauss processes with 100 points, where c is the parameter that controls the strength of interaction and R is the range, in a unit square by the translational edge-correction and the isotropic edge-correction with eight weight functions (———, w_0; · · · · ·, w_1; ———, w_2; ———, w_3; ———, w_4; – – –, w_5; – – –, w_6; – – –, w_7).

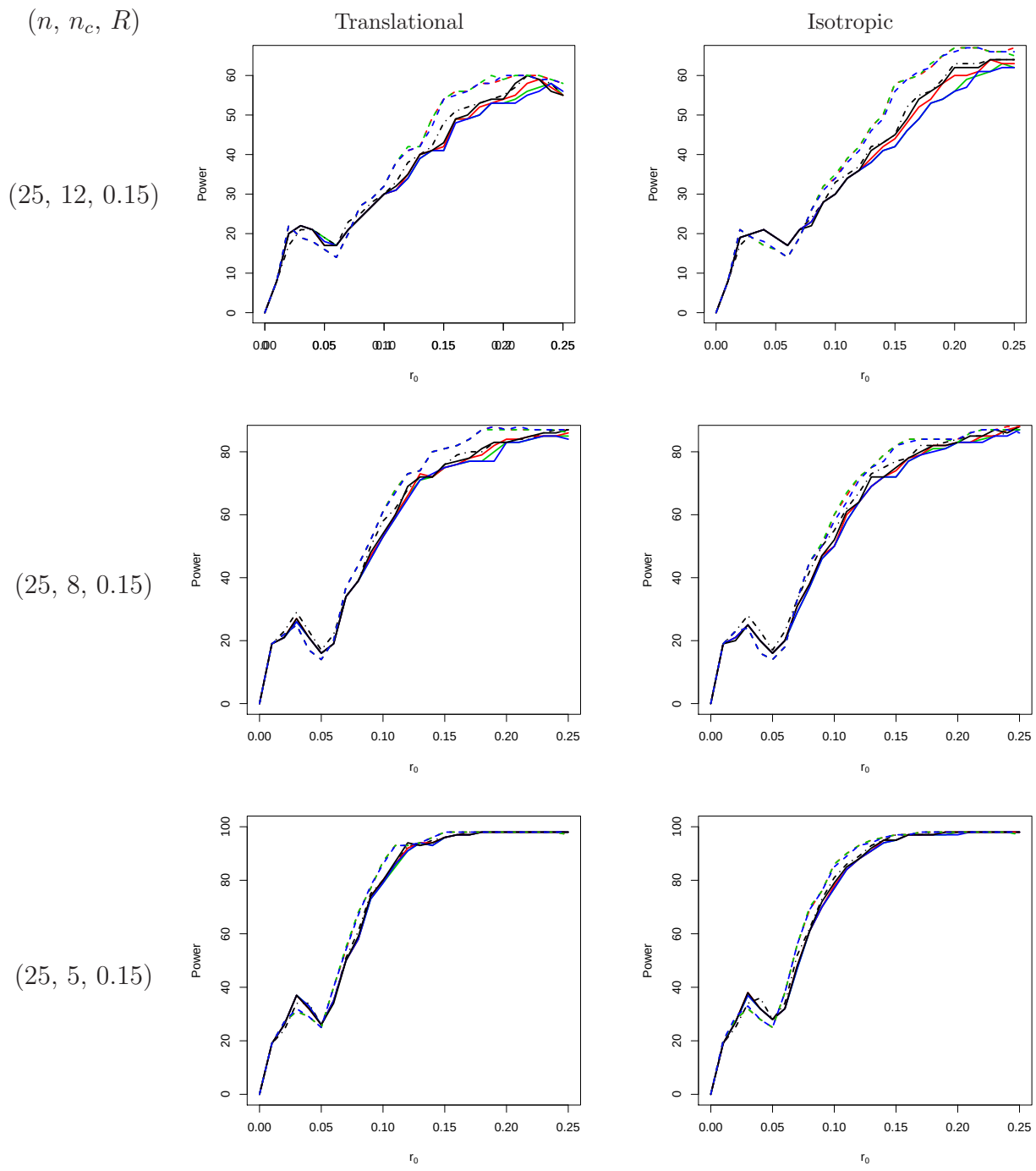

Figure 5: Estimated power (in percent) of the integral statistic for testing CSR against cluster processes that generate 25 points uniformly in n_c circular clusters with radius R in a unit square by the translational edge-correction and the isotropic edge-correction with eight weight functions (——, w_0; · · · · ·, w_1; ——, w_2; ——, w_3; ——, w_4; – – –, w_5; – – –, w_6; – – –, w_7).

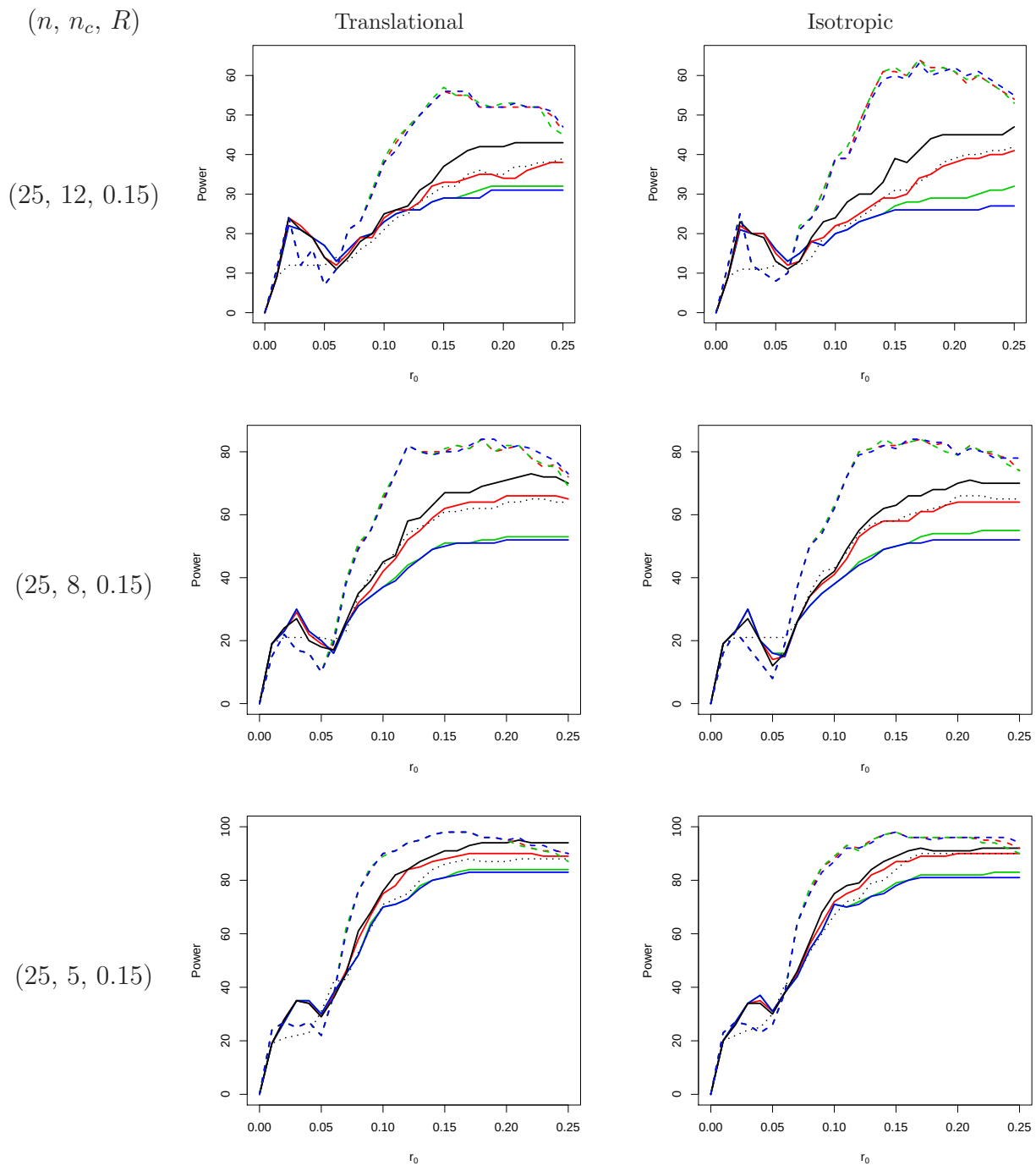

Figure 6: Estimated power (in percent) of the maximum statistic for testing CSR against cluster processes that generate 25 points uniformly in n_c circular clusters with radius R in a unit square by the translational edge-correction and the isotropic edge-correction with eight weight functions (——, w_0; · · · · ·, w_1; ——, w_2; ——, w_3; ——, w_4; – – –, w_5; – – –, w_6; – – –, w_7).

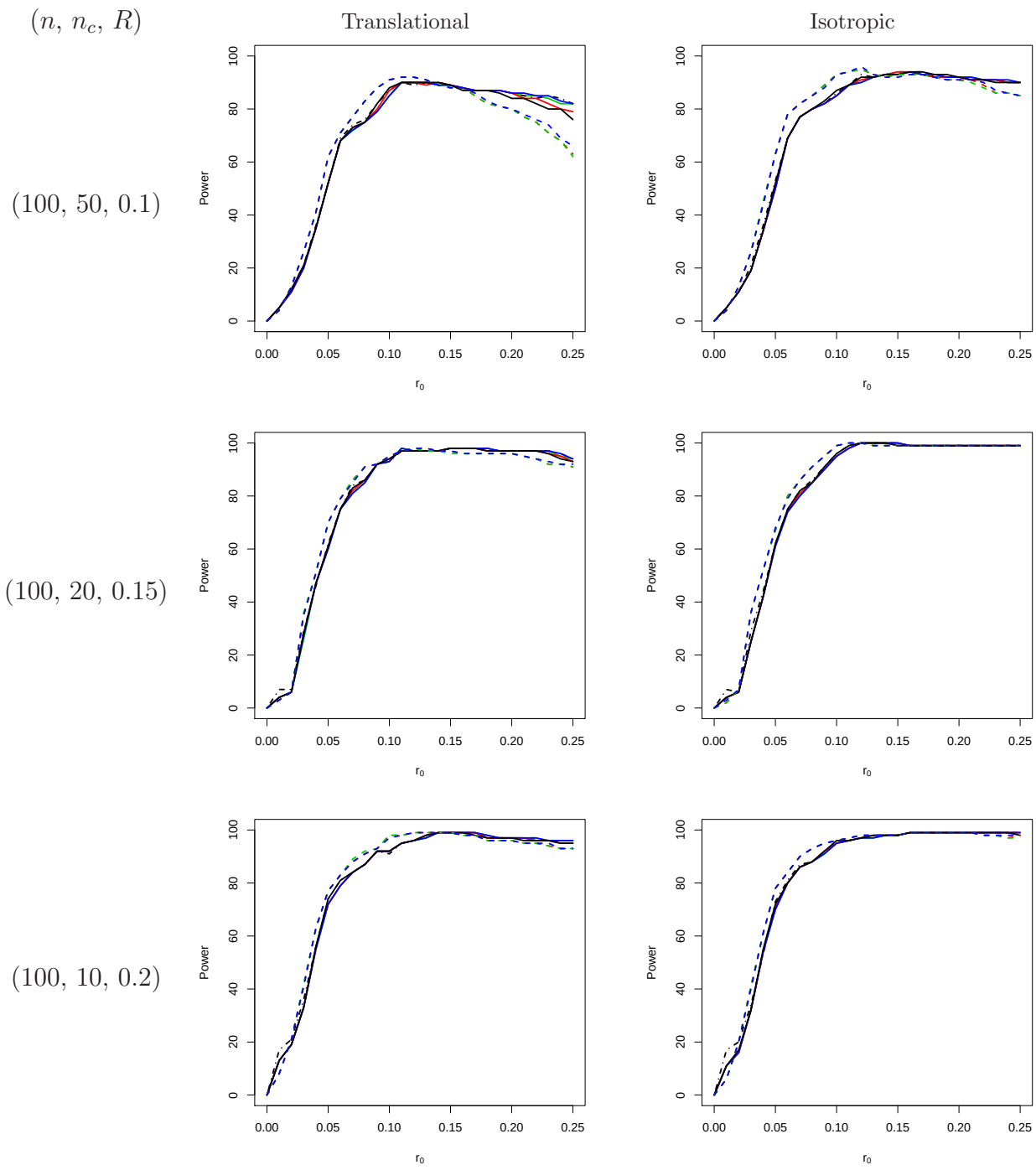

Figure 7: Estimated power (in percent) of the integral statistic for testing CSR against cluster processes that generate 100 points uniformly in n_c circular clusters with radius R in a unit square by the translational edge-correction and the isotropic edge-correction with eight weight functions (——, w_0; · · · · ·, w_1; ——, w_2; ——, w_3; ——, w_4; – – –, w_5; – – –, w_6; – – –, w_7).

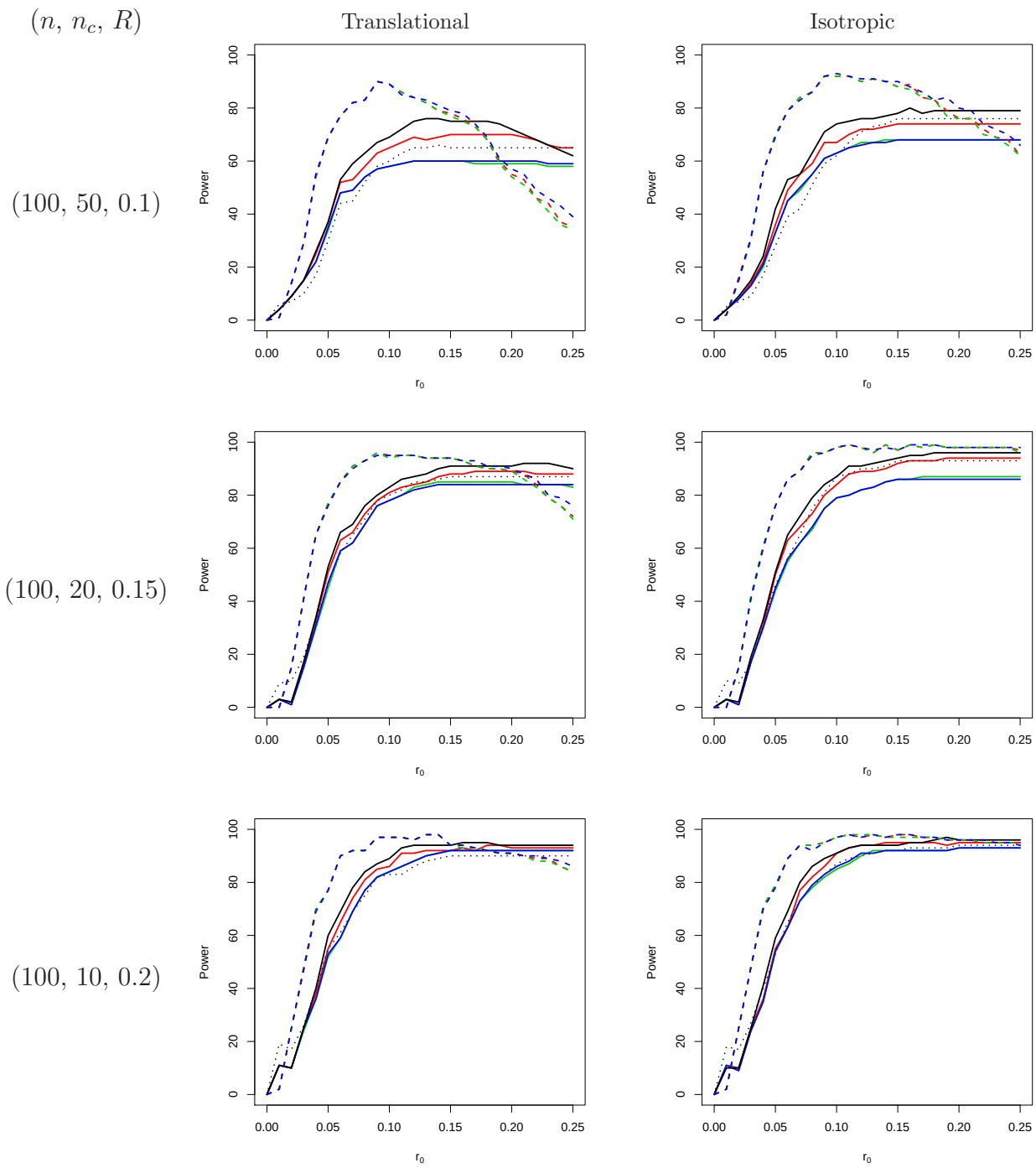

Figure 8: Estimated power (in percent) of the maximum statistic for testing CSR against cluster processes that generate 100 points uniformly in n_c circular clusters with radius R in a unit square by the translational edge-correction and the isotropic edge-correction with eight weight functions (——, w_0; · · · · ·, w_1; ——, w_2; ——, w_3; ——, w_4; – – –, w_5; – – –, w_6; – – –, w_7).

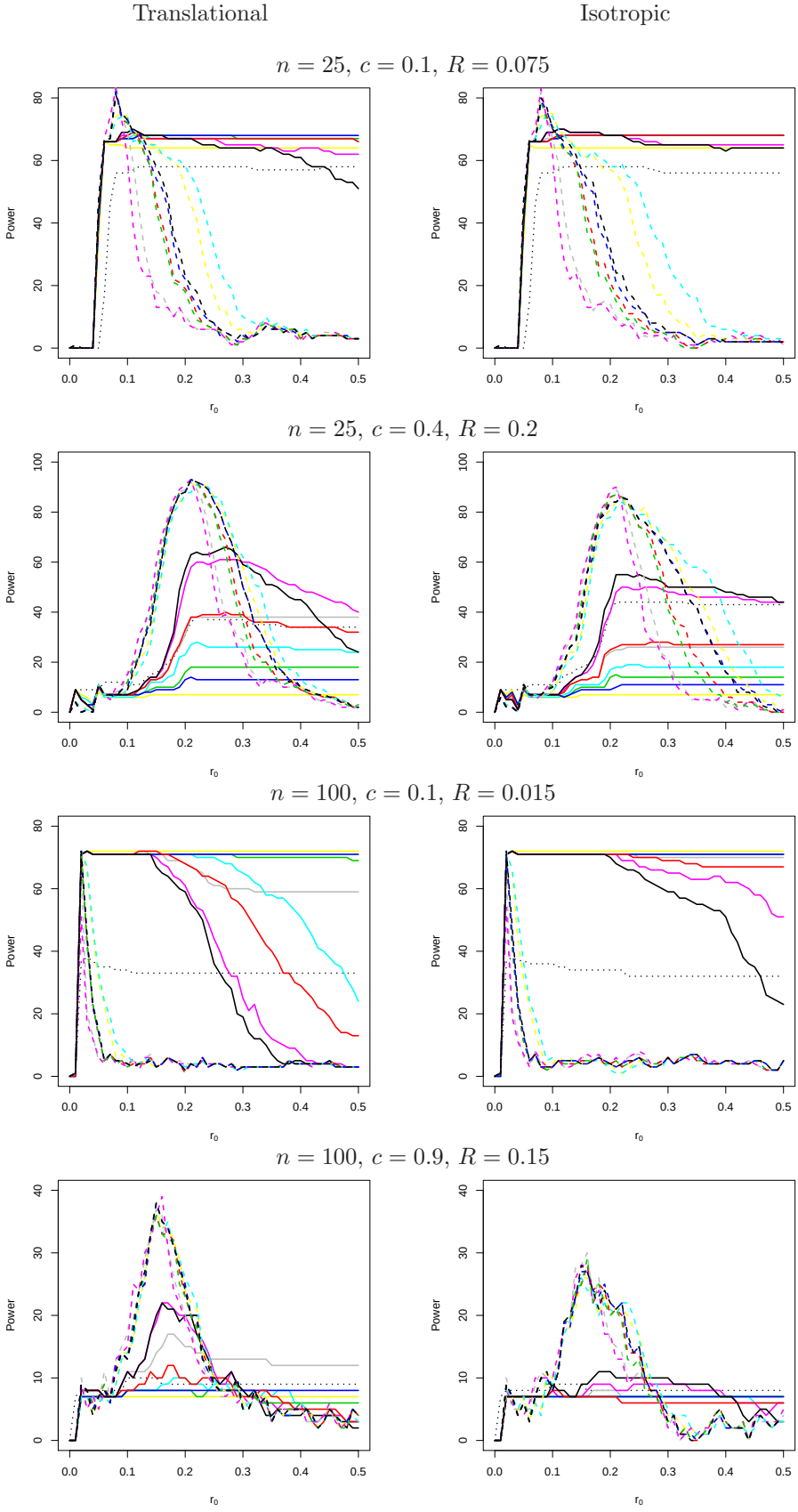
Translational
Isotropic
$n = 25,\ c = 0.1,\ R = 0.075$
$n = 25,\ c = 0.4,\ R = 0.2$
$n = 100,\ c = 0.1,\ R = 0.015$
$n = 100,\ c = 0.9,\ R = 0.15$
Power
r_0

Figure 9:

Figure 9: Estimated power (in percent) of the maximum statistic for testing CSR against Strauss processes with 25 and 100 points, where c is the parameter that controls the strength of interaction and R is the range, in a unit square by the translational edge-correction and the isotropic edge-correction with seventeen weight functions (———, w_0; · · · · ·, w_1; ———, w_2; ———, w_3; ———, w_4; – – –, w_5; – – –, w_6; – – –, w_7; ———, w_8; ———, w_9; ———, w_{10}; ———, w_{11}; – – –, w_{12}; – – –, w_{13}; – – –, w_{14}; – – –, w_{15}; – – –, w_{16}.)

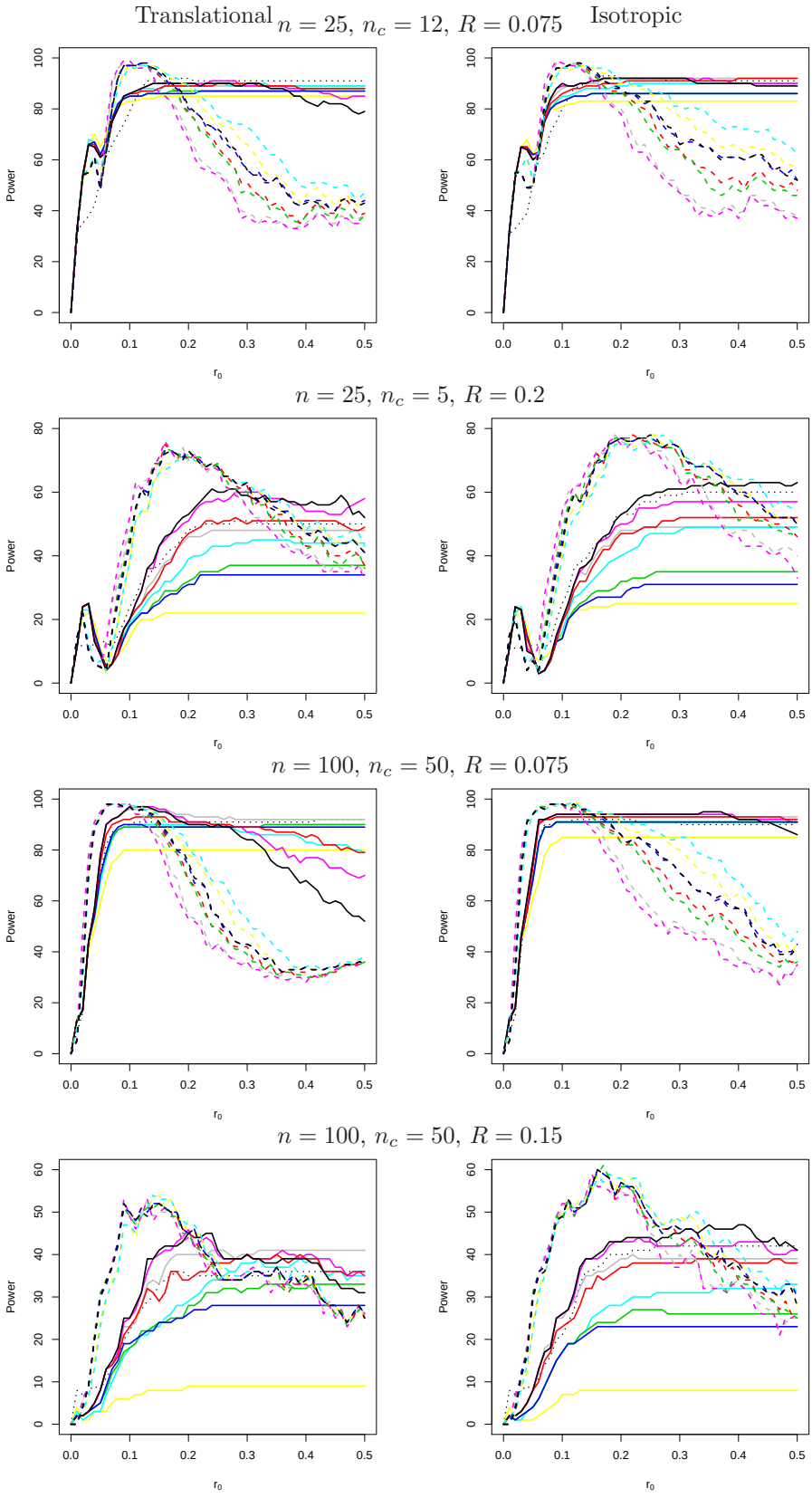
Translational
$n = 25,\ n_c = 12,\ R = 0.075$
Isotropic
Power
r_0
$n = 25,\ n_c = 5,\ R = 0.2$
$n = 100,\ n_c = 50,\ R = 0.075$
$n = 100,\ n_c = 50,\ R = 0.15$

Figure 10:

Figure 10: Estimated power (in percent) of the maximum statistic for testing CSR against cluster processes that generate 25 and 100 points uniformly in n_c circular clusters with radius R in a unit square by the translational edge-correction and the isotropic edge-correction with seventeen weight functions (——, w_0; · · · · ·, w_1; ——, w_2; ——, w_3; ——, w_4; – – –, w_5; – – –, w_6; – – –, w_7; ——, w_8; ——, w_9; ——, w_{10}; ——, w_{11}; – – –, w_{12}; – – –, w_{13}; – – –, w_{14}; – – –, w_{15}; – – –, w_{16}).

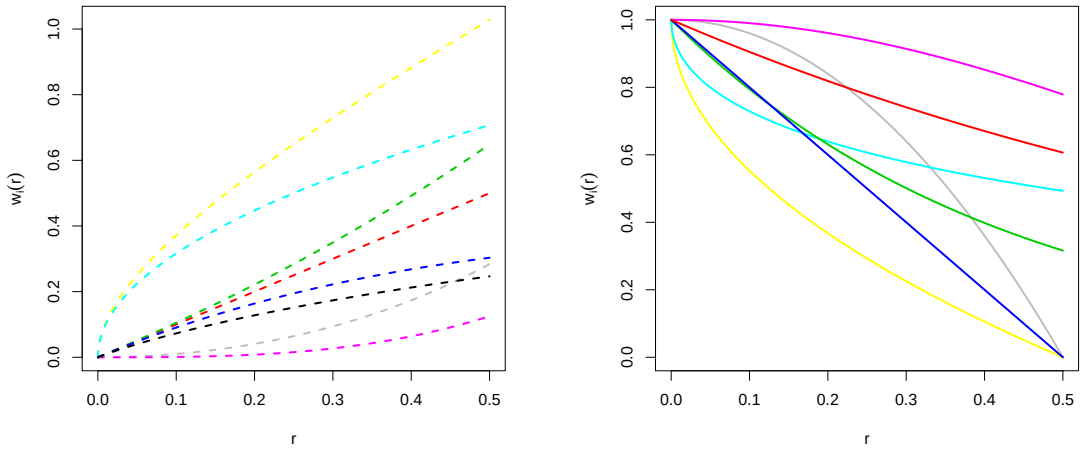

Figure 11: (a) Plots of eight increasing weight functions; (b) Plots of seven decreasing weight function mentioned in text. (——, w_2; ——, w_3; ——, w_4; – – –, w_5; – – –, w_6; – – –, w_7; ——, w_8; ——, w_9; ——, w_{10}; ——, w_{11}; – – –, w_{12}; – – –, w_{13}; – – –, w_{14}; – – –, w_{15}; – – –, w_{16}).

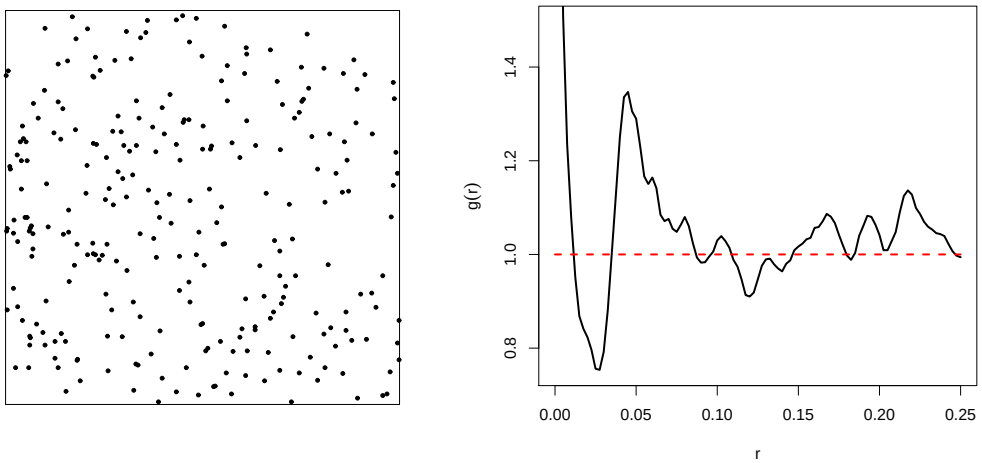

Figure 12: (a) The locations of 270 trees in the south-east Central Russia (Smirnova, 1994); (b) its estimated pair correlation function.

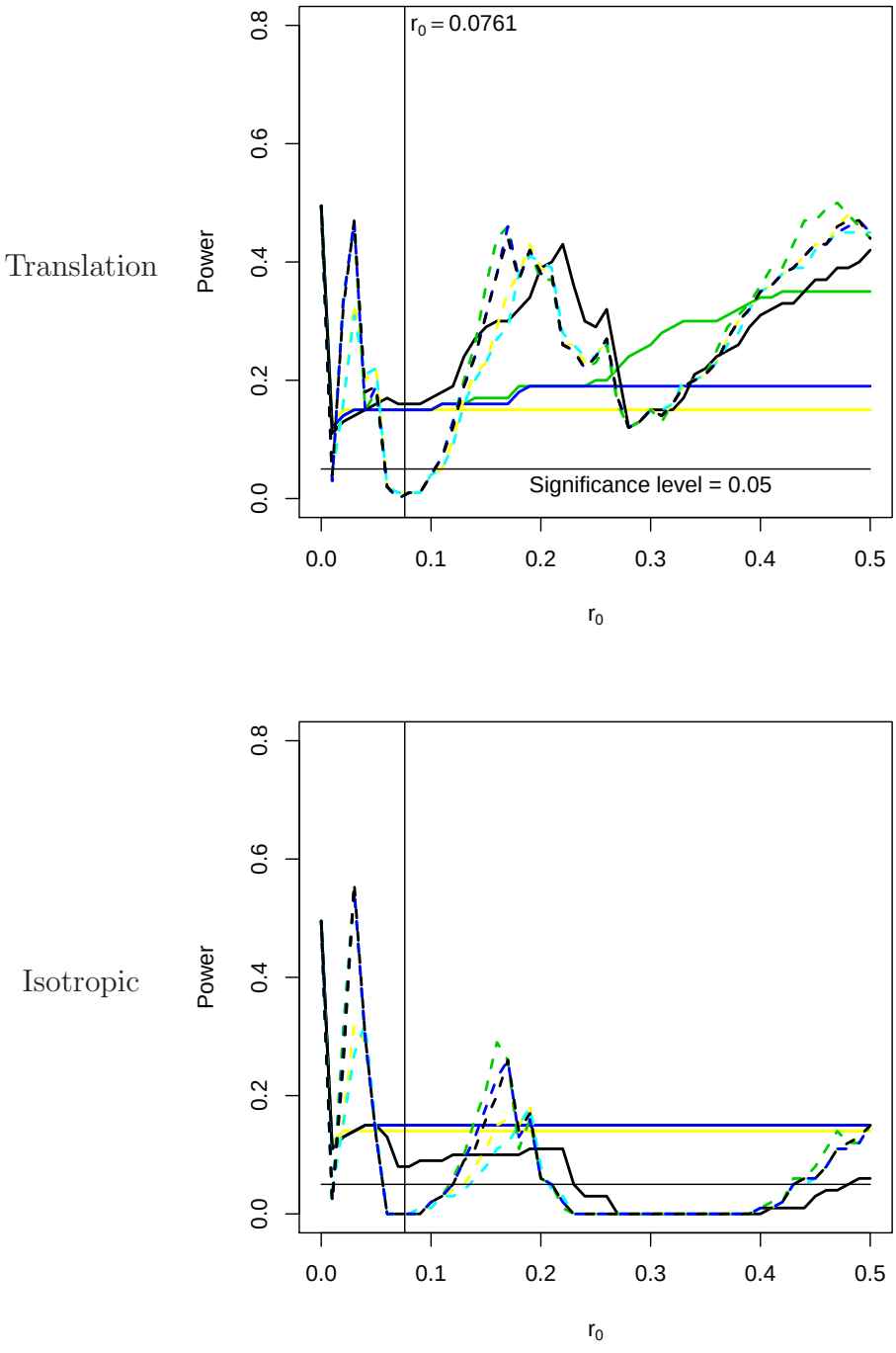

Figure 13: Estimated p-value for testing CSR of the locations of 270 trees in the south-east Central Russia (Smirnova, 1994) by the translational edge-correction and the isotropic edge-correction with eight weight functions (——, w_0; ——, w_3; ——, w_4; – – –, w_7; —— w_{10}; – – –, w_{12}; – – –, w_{14}; – – –, w_{16}).